CYP86A33-Targeted Gene Silencing in Potato Tuber Alters Suberin Composition, Distorts Suberin Lamellae, and Impairs the Periderm's Water Barrier Function[1][C][W][OA]

Olga Serra, Marçal Soler, Carolin Hohn, Vincent Sauveplane, Franck Pinot, Rochus Franke, Lukas Schreiber, Salomé Prat, Marisa Molinas, and Mercè Figueras*

Laboratori del Suro, Departament de Biologia, Facultat de Ciències, Universitat de Girona, E–17071 Girona, Spain (O.S., M.S., M.M., M.F.); Institute of Cellular and Molecular Botany, University of Bonn, D–53115 Bonn, Germany (C.H., R.F., L.S.); CNRS, Université Louis Pasteur, Institut de Biologie Moléculaire des Plantes, F–67083 Strasbourg, France (V.S., F.P.); and Centro Nacional de Biotecnología, Consejo Superior de Investigaciones Científicas, Campus Universidad Autónoma de Madrid, E–28049 Madrid, Spain (S.P.)

Suberin is a cell wall lipid polyester found in the cork cells of the periderm offering protection against dehydration and pathogens. Its biosynthesis and assembly, as well as its contribution to the sealing properties of the periderm, are still poorly understood. Here, we report on the isolation of the coding sequence *CYP86A33* and the molecular and physiological function of this gene in potato (*Solanum tuberosum*) tuber periderm. *CYP86A33* was down-regulated in potato plants by RNA interference-mediated silencing. Periderm from *CYP86A33*-silenced plants revealed a 60% decrease in its aliphatic suberin load and greatly reduced levels of C18:1 ω-hydroxyacid (approximately 70%) and α,ω-diacid (approximately 90%) monomers in comparison with wild type. Moreover, the glycerol esterified to suberin was reduced by 60% in the silenced plants. The typical regular ultrastructure of suberin, consisting of dark and light lamellae, disappeared and the thickness of the suberin layer was clearly reduced. In addition, the water permeability of the periderm isolated from *CYP86A33*-silenced lines was 3.5 times higher than that of the wild type. Thus, our data provide convincing evidence for the involvement of ω-functional fatty acids in establishing suberin structure and function.

Periderm, the boundary tissue that replaces the epidermis in the secondary organs of plants, provides efficient protection against dehydration, UV radiation, and pathogens (Esau, 1965). Periderm is regularly found in the bark of woody plants, but herbaceous plants may also form a well-developed periderm in roots, tubers, and the oldest portions of stem. The periderm has been widely studied in potato (*Solanum tuberosum*) tubers because of the latter's great agronomic significance (Schmidt and Schönherr, 1982; Vogt et al., 1983; Lulai and Freeman, 2001; Sabba and Lulai, 2002). Shrinkage and flaccidity occur in tubers if the protection afforded by the periderm against water loss is compromised (Lulai et al., 2006). Suberin and waxes embedded into the suberin matrix are considered essential for periderm imperviousness (Franke and Schreiber, 2007). Chemically, suberin is a complex lipid polymer consisting of a fatty acid-derived domain (aliphatic suberin) cross-linked by ester bonds to a polyaromatic lignin-like domain (aromatic suberin; Kolattukudy, 2001; Bernards, 2002; Franke and Schreiber, 2007). Aliphatic suberin has been widely analyzed in potato periderm (Kolattukudy and Agrawal, 1974; Graça and Pereira, 2000; Schreiber et al., 2005). The main monomers released from potato aliphatic suberin are a mixture of ω-hydroxyacids and α,ω-diacids with chain lengths ranging from C16 to C28 (mainly C18), together with glycerol. Small amounts of monofunctional fatty acids, alcohols, and ferulic acid are also released. Waxes are complex mixtures of lipids extractable with chloroform that in potato periderm consist mostly of linear very-long-chain aliphatics up to C32 (Schreiber et al., 2005). Suberin is deposited in the cell wall as a continuous deposit or secondary cell wall that overlays the polysaccharide primary cell wall from the inside (Esau, 1965). These suberin deposits appear under the transmission electron microscope (TEM) as regularly alternating opaque

[1] This work was supported by the Spanish Ministerio de Ciencia y Tecnología (grant no. AGL2003–00416); the Ministerio de Educación y Ciencia (grant no. AGL2006–07342, an FPI grant, and two mobility grants to O.S.); the Departament d'Universitats, Investigació i Societat de la Informació of Catalonia and European Social Fund (FI grant to M.S.); and the Deutsche Forschungsgemeinschaft.

* Corresponding author; e-mail merce.figueras@udg.edu.

The author responsible for distribution of materials integral to the findings presented in this article in accordance with the policy described in the Instructions for Authors (www.plantphysiol.org) is: Mercè Figueras (merce.figueras@udg.edu).

[C] Some figures in this article are displayed in color online but in black and white in the print edition.

[W] The online version of this article contains Web-only data.

[OA] Open access articles can be viewed online without a subscription.

www.plantphysiol.org/cgi/doi/10.1104/pp.108.127183

and translucent lamellae (Schmidt and Schönherr, 1982). Although several molecular models for suberin have been proposed (Kolattukudy, 1980; Bernards, 2002; Graça and Santos, 2007), how the suberin and wax components are organized in the lamellated suberin secondary cell wall is a matter of debate (Graça and Santos, 2007). Moreover, to what extent suberin and wax deposition and composition determine sealing properties of periderm still remains unclear (Schreiber et al., 2005). Several studies confirm the importance of waxes for the diffusion barrier (Soliday et al., 1979; Vogt et al., 1983; Schreiber et al., 2005), but the significance of aliphatic suberin has hardly been investigated at all. Interestingly, an Arabidopsis (*Arabidopsis thaliana*) knockout mutant for the *GLYCEROL-3-PHOSPHATE ACYLTRANSFERASE5* gene (*GPAT5*) with altered suberin showed higher tetrazolium salt permeability in the seed coat (Beisson et al., 2007).

ω-Hydroxylation of fatty acids, a reaction carried out in plants by cytochrome P450 monooxygenases, is a crucial step in the biosynthesis of plant biopolymers (Kolattukudy, 1980; Nawrath, 2002). The Arabidopsis mutant *lacerata*, which shows phenotype defects compatible with a cutin deficiency, is defective in *CYP86A8* encoding a fatty acid ω-hydroxylase (Wellesen et al., 2001). The *aberrant induction of type three genes1* (*att1*) mutant, showing an altered cuticle ultrastructure and a higher transpiration rate than wild type, is defective in *CYP86A2* and contains reduced amounts of ω-functionalized cutin monomers (Xiao et al., 2004). Moreover, a genome-wide study of cork oak (*Quercus suber*) bark highlighted a member of the cytochrome P450 of the CYP86A subfamily as a strong candidate gene for aliphatic suberin biosynthesis (Soler et al., 2007); and a role for *CYP86A1* in the biosynthesis of suberin has recently been confirmed in the primary root of Arabidopsis knockout mutants (Li et al., 2007; Hofer et al., 2008). However, how the lack of fatty acid ω-hydroxylase activity may affect the structural features and sealing properties of suberin in periderm cell walls has not been documented.

To provide experimental evidence of the role of *CYP86A* genes in periderm fine structure and water transpiration properties, especially quantitative permeability studies so far unexplored in Arabidopsis, we followed a strategy based on the potato (cv *Desirée*). The potato is a model of choice for such studies because transgenic plants can be produced in reasonable time and sufficient amounts of periderm can easily be obtained from tubers for chemical and physiological studies (Vogt et al., 1983; Schreiber et al., 2005). Based on the *CYP86A* gene that was highlighted in cork oak periderm as a strong suberin candidate for aliphatic suberin biosynthesis, we isolated the putative ortholog in potato and used a reverse genetic approach to analyze the effects of down-regulation on the chemical and ultrastructural features of suberin and on the physiological properties of the tuber periderm. Our findings indicate that down-regulation of *CYP86A33*, as this gene was designated, results in a strong decrease of the ω-functionalized monomers in aliphatic suberin, which are necessary for the suberin typical lamellar organization and for the periderm resistance to water loss.

RESULTS

Cloning and Phylogenetic Analysis of Potato CYP86A33 and Cork Oak CYP86A32

We obtained the full-length coding sequence of a cork oak *CYP86A* gene (accession no. EU293406) highlighted by prior works as a strong candidate for suberin biosynthesis (Soler et al., 2007, 2008). This gene, henceforth referred to as *CYP86A32*, was then used as a query to identify the potato homologous sequence in The Institute for Genomic Research (TIGR; http://www.tigr.org) database. Highest homology (86% similarity) was for potato tentative consensus TC148994, which was assembled from tuber and root ESTs. Although TC148994 covered a complete coding sequence, no true open reading frame was obtained. Thus, cDNA prepared from potato tuber skin was used to isolate the complete coding sequence (accession no. EU293405), referred to as *CYP86A33*. The amino acid sequences of CYP86A32 and CYP86A33 displayed high similarity (88% and 89%, respectively) to Arabidopsis CYP86A1.

A phylogenetic study with the CYP86A subfamily in Arabidopsis and rice (*Oryza sativa*) was carried out to trace the phylogenetic position of CYP86A32 and CYP86A33 among the CYP86A subfamily. All Arabidopsis proteins included in the study demonstrated in vitro ω-hydroxylase activity (Benveniste et al., 1998; Kandel et al., 2007; Rupasinghe et al., 2007) and also—for CYP94C1—a capacity to yield α,ω-diacids (Kandel et al., 2007). A multiple amino acid sequence alignment generated by ClustalW was used to generate two unrooted phylogenetic trees using, respectively, the neighbor-joining and the unweighted pair group method with arithmetic mean algorithms. Both returned identical clade distributions with similar bootstrap values (Fig. 1A). Arabidopsis CYP86A1, cork oak CYP86A32, and potato CYP86A33 (bootstrap value ≥ 980/1,000) together with rice CYP86A9 (bootstrap value ≥ 870/1,000) fell into the same subclade. All the other members of the CYP86A subfamily grouped according to paralogous relationships as shown by prior phylogenetic analyses (Nelson et al., 2004; Duan and Schuler, 2005). CYP94C1 was excluded from the CYP86A clade. The amino acid sequence alignment of CYP86A32, CYP86A33, and the two most homologous proteins, CYP86A1 and CYP86A9, showed high sequence conservation (Fig. 1B), including residues predicted to contact oleic acid in Arabidopsis CYP86A proteins (Rupasinghe et al., 2007). Conservation was more pronounced in the sequence region ranging from the substrate recognition site 4 (SRS4) to the C-terminal end.

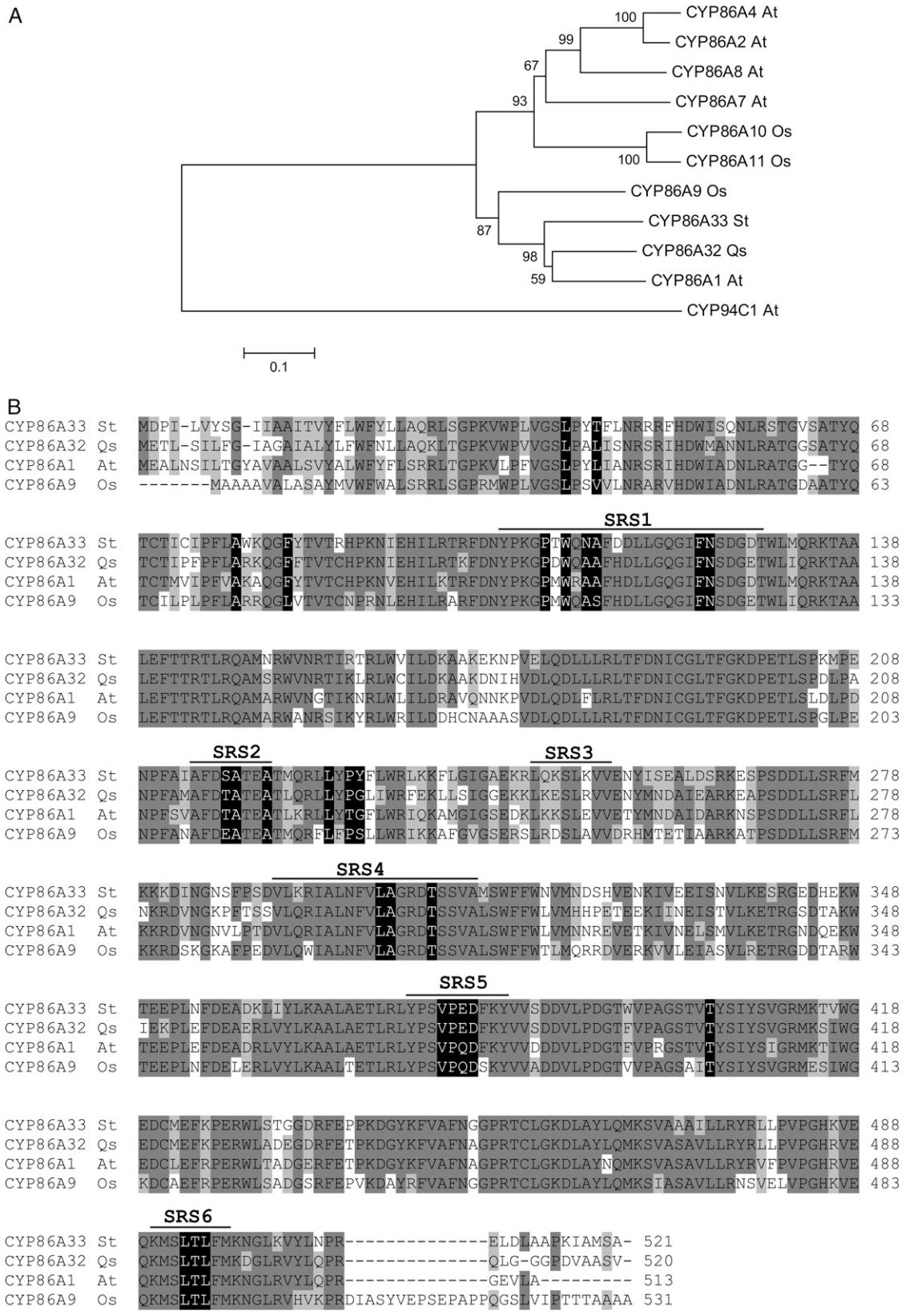

Figure 1. Phylogenetic analysis of CYP86A subfamily members. A, Phylogenetic analysis of CYP86A32 and CYP86A33. Amino acid sequences of *Q. suber* (Qs) CYP86A32 and *S. tuberosum* (St) CYP86A33 were aligned by ClustalW with the CYP86A protein

CYP86A33 Tissue Specificity and Down-Regulation in Potato

A northern-blot analysis to verify the expression pattern of *CYP86A33* in potato tissues prior to RNA interference (RNAi) silencing revealed marked tissue and organ specificity (Fig. 2A). The transcript accumulated heavily in the periderm (tuber skin) and in smaller amounts in the primary root, with both containing suberin. No expression could be detected in stem, leaf, or tuber parenchyma.

To prevent the silencing of off-target genes, the *CYP86A33* RNAi-mediated silencing in potato was performed using a nonconserved region of 224 bp, identified by BLASTN analysis (Altschul et al., 1990) against the most similar sequences in TIGR potato database. Double insertion of this gene region into the pBIN19RNAi vector using Gateway LR clonase generated an inverted repeat construct capable of producing a hairpin chimera that targets the *CYP86A33* mRNA. Transgenic plants were produced by *Agrobacterium*-mediated transformation. Twenty-nine kanamycin-resistant lines from independent transformation events were grown in the greenhouse until tuber harvesting. Northern-blot analysis of the tuber skin identified 14 of these lines (48%) as effectively silenced. Gene silencing was reconfirmed in three lines (Fig. 2B) that were propagated to produce enough tubers to analyze the chemical composition and water permeability of the periderm. For data presented here, tubers were harvested from 8-week-old plants and stored for 21 d at room temperature before periderm analysis.

To identify putative unintended targets of *CYP86A33* silencing, a BLASTN analysis in TIGR potato database (http://compbio.dfci.harvard.edu/tgi/cgi-bin/tgi/gimain.pl?gudb=potato) was performed using the *CYP86A33*-RNAi fragment as a query. The most homologous ESTs are TC175254 and BQ514437 (64% similarity), which have maximal similarity to Arabidopsis CYP86A2 and CYP96A9, respectively (Supplemental Table S1). According to microarray experiments in TIGR Solanaceae Genomics Resource (http://www.tigr.org/tdb/sol), these two genes are highly expressed in tuber skin and the *CYP86A9* putative ortholog is also induced during tuber onset just as *CYP86A33*. On the other hand, TC175254 and BQ514437 alignment with the *CYP86A33*-RNAi fragment (Supplemental Fig. S1A) shows that BQ514437 has a longer sequence with high identity (92% identity from 174–200 nucleotides of RNAi fragment) and therefore a higher probability of being RNAi off-target exists. To check whether the transcripts of this gene could be off-targets of *CYP86A33* short-interfering RNA, its mRNA level was analyzed by means of a reverse transcription (RT)-PCR analysis in parallel with those of *ACTIN* and *CYP86A33*. Results showed that, whereas the levels of *CYP86A33* transcript are lower in *CYP86A33*-silenced lines, those of BQ514437 are not affected by silencing (Supplemental Fig. S1B). Taking into account this result and the information available in potato databases, there is no cross-silencing and therefore we can assume that the phenotype observed in *CYP86A33*-silenced lines must be a consequence of CYP86A33 deficiency.

CYP86A33 Down-Regulation and Suberin Fine Structure

Potato plants silenced for *CYP86A33* developed normally either in vitro or in pots. No phenotypic changes could be observed in leaves, shoots, roots, or developing tubers when compared to wild-type plants. Neither when freshly harvested nor during postharvesting storage at room temperature did the tubers from *CYP86A33*-silenced plants show a different phenotype in comparison to wild type. Only when the period of storage was greater than 2 months did tubers deficient in CYP86A33 appear somewhat more wrinkled than wild type (Fig. 3A). The anatomy and fine structure of the periderm was analyzed in 21-d-stored tubers. Examining the periderm using light and fluorescence microscopy did not reveal obvious differences in the general cellular architecture between wild-type and *CYP86A33*-silenced tubers. Neither did a more detailed observation using scanning electron microscopy (SEM) show any obvious difference (Fig. 3B). However, for *CYP86A33*-silenced periderm TEM analysis revealed a pronounced reduction in the thickness of the suberin or secondary wall and a deep alteration in the suberin ultrastructure (Fig. 3C) as compared to wild type (Fig. 3D). In *CYP86A33*-silenced periderm cell walls, the typical regular lamellation of the suberin layer disappeared, whereas the electron-translucent and electron-dense material formed prominent clumps and thick lamellar deposits (Fig. 3C, white arrows). The surface of the suberin

Figure 1. (*Continued.*)
subfamily of Arabidopsis (At) CYP86A1, CYP86A2, CYP86A4, CYP86A7, and CYP86A8 and rice (*Oryza sativa*; Os) CYP86A9, CYP86A10, and CYP86A11. A CYP94 family member (CYP94C1) was also added. Alignment was used to construct a neighbor-joining tree using the MEGA package, version 3.1. Identical clade distribution and similar bootstrap values were obtained using an unweighted pair group method with arithmetic mean algorithm. Bootstrapped values indicating the level of significance (%) by the separation of the branches are shown. The branch length indicates the extent of the difference according to the scale at the bottom. Note that CYP86A1, CYP86A32, CYP86A33, and CYP86A9 are grouped within the same subclade, although CYP86A9 is separated from the rest. CYP86A and CYP94 are clearly separated in two major clades as previously reported. B, Amino acid sequence alignment of the related proteins CYP86A32, CYP86A33, CYP86A1, and CYP86A9. Amino acids that are identical or similar are shaded in dark or light gray, respectively. SRSs are underlined, and the residues, which it is predicted will contact the oleic acid substrate, are shaded in black.

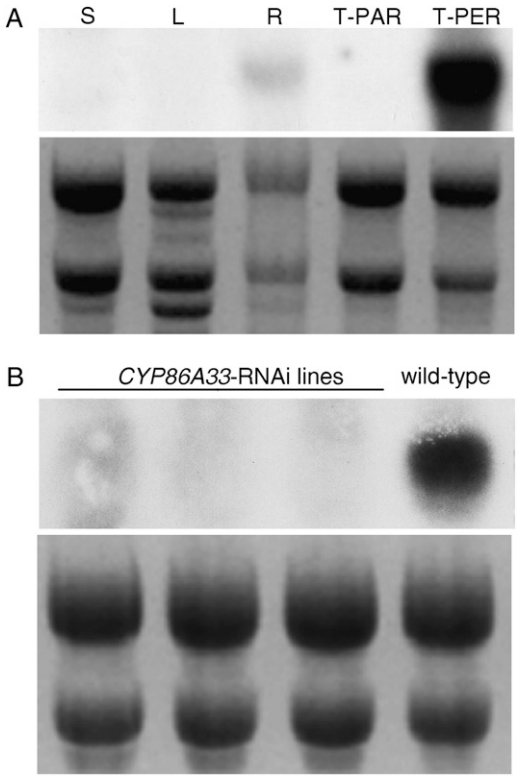

Figure 2. Northern-blot analysis of *CYP86A33* in potato organs and tuber tissues. Northern-blot membranes and ethidium bromide-stained gels are shown in the upper and lower panels of each image, respectively. A, Transcript profile in potato: stem (S), leaf (L), root (R), tuber parenchyma (T-PAR), and tuber periderm (T-PER). Note that the *CYP86A33* transcript accumulates only in suberized tissues: roots and tuber periderm. B, Transcript accumulation in tuber periderms of three independent *CYP86A33*-RNAi transgenic potato plants in comparison to wild type. Periderms from these three lines were selected for chemical and water permeability analyses.

layer in contact with the tertiary polysaccharide wall appeared uneven. Some cell walls, but not all, showed bulges or folds affecting the suberin layer and the tertiary wall (Fig. 3C, arrowhead).

CYP86A33 Down-Regulation and Periderm Lipid Composition

The chemical composition of the soluble (wax) and insoluble (suberin) aliphatic fractions was analyzed by gas chromatography (GC) in periderm from the three independent *CYP86A33* down-regulated lines (Fig. 2B). Periderm was enzymatically isolated as detailed in "Materials and Methods." For chemical analysis, the wax fraction was extracted by organic solvent and the remaining suberin polyester analyzed after transesterification.

Enzymatically isolated periderm from *CYP86A33*-silenced tubers had a more fragile appearance, breaking easily when handled and, once dried, it was about 50% lighter than wild type (*CYP86A33*-RNAi 1.80 ± 0.23 mg cm^{-2}, wild-type 2.69 ± 0.23 mg cm^{-2}). The aliphatic suberin, which is the main lipid fraction accounting for 96% of the total lipids in wild-type periderm, was greatly affected by CYP86A33 deficiency. As measured in periderm from 21-d-stored tubers, total aliphatic suberin amounted to 462.27 ± 69.93 μg cm^{-2} in wild type, but only 180.88 ± 22.38 μg cm^{-2} in *CYP86A33*-silenced periderm, a reduction of 60%. All monomers showed a significant decrease (Fig. 4). The greatest reduction was in ω-hydroxyacids (Fig. 4B) and α,ω-diacids as a whole (Fig. 4C). Specifically, C18:1 α,ω-diacid and ω-hydroxyacid were reduced by 90% and 70%, respectively; C20:0 ω-hydroxyacid and C18:0 α,ω-diacid were also signif-

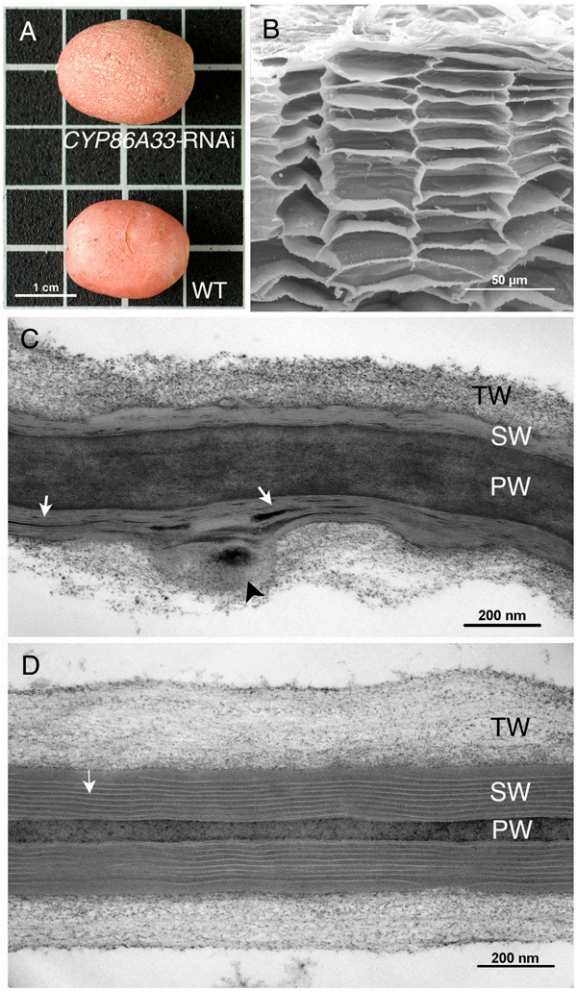

Figure 3. Anatomy and fine structure of periderms of *CYP86A33*-RNAi tubers. A, Wild-type (WT) and *CYP86A33*-silenced tubers. B, SEM sections of the down-regulated periderm reveals a normal organization of the cell layers as in wild-type periderm (not shown). C, TEM micrograph of the suberized cell wall of *CYP86A33*-RNAi peridermal cells. D, TEM micrograph of the suberized cell wall of wild-type peridermal cells. PW, Primary wall; SW, secondary suberin wall; TW, tertiary wall; white arrows, suberin lamellation; black arrowhead, atypical structures consisting of bulges or folds in the suberin wall. [See online article for color version of this figure.]

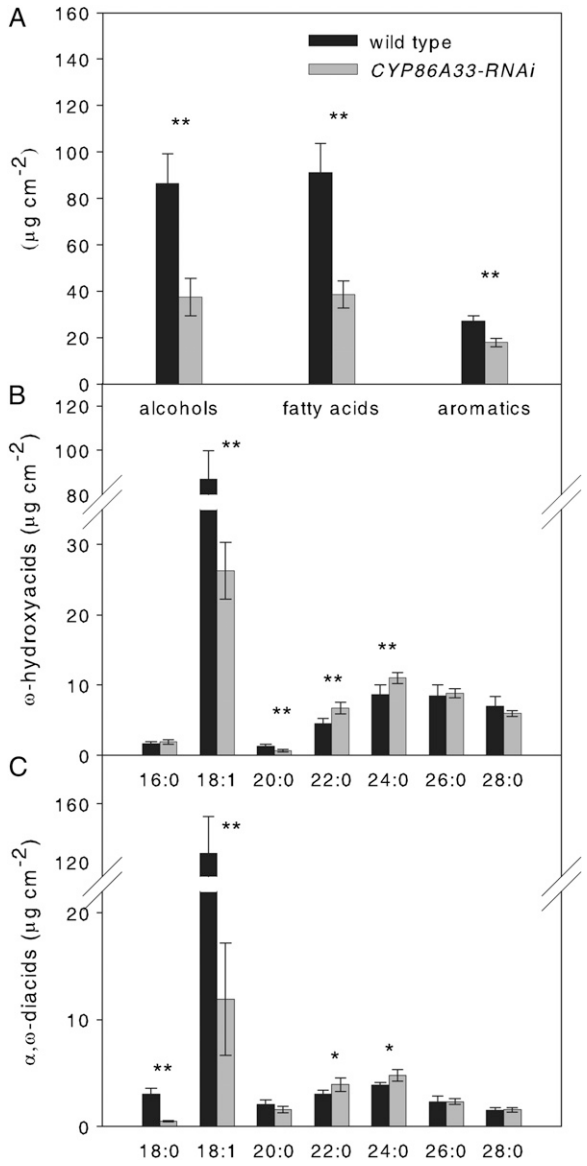

Figure 4. Aliphatic suberin chemical composition of wild-type and *CYP86A33*-RNAi periderms from 21-d-stored tubers. A, Total amounts of primary alcohols, fatty acids, and aromatic compounds. B, All ω-hydroxyacid monomers identified. C, All α,ω-diacid monomers identified. Asterisks denote a significant difference between *CYP86A33*-RNAi ($n = 6$) and wild-type ($n = 4$) periderms (*t* test; *, $P < 0.05$; **, $P < 0.01$). Data are represented as an average of three independent *CYP86A33*-RNAi lines. Data represent the mean ± SD.

icantly reduced; C22:0 and C24:0 ω-hydroxyacids and α,ω-diacids showed a very minor, but statistically significant, increase. Glycerol was reduced by 60% (from 63.57 ± 19.79 μg cm^{-2} in wild type to 25.89 ± 13.84 μg cm^{-2} in *CYP86A33* down-regulated periderm). In contrast with suberin, the wax fraction (4% of total lipids in wild type) was increased by a factor of 2.4 in the *CYP86A33*-RNAi periderm (Table I). The increase was higher in free fatty acids and ferulic acid esters (a 3.4-fold increase), whereas alkanes and alcohols showed only minor changes (Table I).

To exclude the possibility that the changes in suberin and wax composition of *CYP86A33* down-regulated plants could be due to a delay in the periderm maturation process, freshly harvested (0-d-stored) and 60-d-stored tubers were analyzed for comparison. For both, the general variation in aliphatic suberin composition between *CYP86A33*-silenced and wild-type tubers (Supplemental Fig. S2) was similar to that observed in 21-d-stored tubers (Fig. 4). Moreover, the aliphatic suberin load was in both freshly harvested and 60-d-stored tubers reduced by 60% and the greatest reductions corresponded to C18:1 ω-hydroxyacids and α,ω-diacids. As regards the wax fraction, the effects of *CYP86A33* knockdown in wax amount and chemical composition were similar in freshly harvested

Table I. *Wax monomer content (μg cm^{-2}) of wild-type (n = 4) and CYP86A33-RNAi periderms (n = 6) from 21-d-stored tubers*

The soluble aliphatic fraction was obtained by treating the enzymatically isolated periderm with 1:1 chloroform:methanol. Absolute amounts of released monomers and the total amount of each substance class are given. Asterisks denote a significant increase (↑) in *CYP86A33*-RNAi periderms compared to wild type (*t* test; *, $P < 0.05$; **, $P < 0.01$). Data are represented as an average of three independent *CYP86A33*-RNAi lines. Data represent the mean ± SD.

	Wax Chemical Composition	
	Wild Type	*CYP86A33*-RNAi
	μg cm^{-2}	μg cm^{-2}
Alkanes		
C25	3.67 ± 2.70	2.92 ± 1.33
C26	0.25 ± 0.19	0.11 ± 0.07
C27	1.00 ± 0.25	2.88 ± 0.52 **↑
Total	4.93 ± 2.98	5.92 ± 1.11
Alcohols		
C26	0.20 ± 0.09	0.48 ± 0.12 **↑
C28	3.31 ± 0.87	2.86 ± 0.37
C30	0.61 ± 0.19	1.31 ± 0.55 *↑
Total	4.12 ± 0.98	4.65 ± 0.42
Fatty acids		
C22:0	0.13 ± 0.10	0.15 ± 0.03
C24:0	0.11 ± 0.05	0.31 ± 0.03 **↑
C26:0	0.11 ± 0.05	0.84 ± 0.18 **↑
C28:0	0.39 ± 0.18	1.70 ± 0.45 **↑
C30:0	0.46 ± 0.22	1.07 ± 0.25 **↑
Total	1.20 ± 0.43	4.06 ± 0.88 **↑
Ferulic acid esters		
C18	0.34 ± 0.20	0.63 ± 0.15 *↑
C20	0.16 ± 0.09	0.51 ± 0.10 **↑
C21	0.28 ± 0.09	2.51 ± 0.45 **↑
C22	0.08 ± 0.03	0.79 ± 0.21 **↑
C23	0.38 ± 0.09	4.93 ± 0.89 **↑
C24	0.13 ± 0.04	1.71 ± 0.47 **↑
C25	0.16 ± 0.05	0.69 ± 0.12 **↑
C26	0.31 ± 0.10	1.75 ± 0.34 **↑
C27	0.14 ± 0.09	0.33 ± 0.05 **↑
C28	1.36 ± 0.53	3.64 ± 0.41 **↑
C29	0.71 ± 0.31	2.08 ± 0.41 **↑
C30	3.34 ± 0.91	7.61 ± 0.85 **↑
C31	0.56 ± 0.35	1.16 ± 0.30 *↑
Total	7.96 ± 2.33	28.32 ± 3.39 **↑
Total waxes	18.21 ± 5.02	42.95 ± 3.08 **↑

and 21-d-stored tubers. For 60-d-stored tubers, the total wax load showed no statistically significant differences compared with wild type.

CYP86A33 Down-Regulation and Periderm Water Permeability

The water permeability of isolated periderm was measured by a gravimetric method in wild type and in the three independent *CYP86A33* down-regulated lines. Water permeance in silenced periderms showed on average a 3.5-fold increase compared with that of wild-type periderm (Fig. 5). Permeance increased significantly from $0.81 \pm 0.26 \times 10^{-10}$ m s^{-1} (mean ± SD) in wild type to an average of $2.82 \pm 0.838 \times 10^{-10}$ m s^{-1}. Similar results were obtained using periderm from 60-d-stored tubers (Supplemental Fig. S3).

DISCUSSION

Results presented here suggest that CYP86A33 is critical for the aliphatic suberin biosynthesis in potato periderm. Decrease on ω-functional fatty acids has strong consequences in the ultrastructural organization and water-sealing properties of suberin. The results are consistent with the fact that *CYP86A33* transcript accumulates only in tissues where suberin is deposited (Fig. 2A). Moreover, our findings agree with the pattern of transcript accumulation during the stolon-to-tuber transition because accumulation begins at tuberization onset, as shown by the microarray hybridization data stored in TIGR Solanaceae genomics resource (http://www.tigr.org/tigr-scripts/tdb/sol/study/sol_expression.pl).

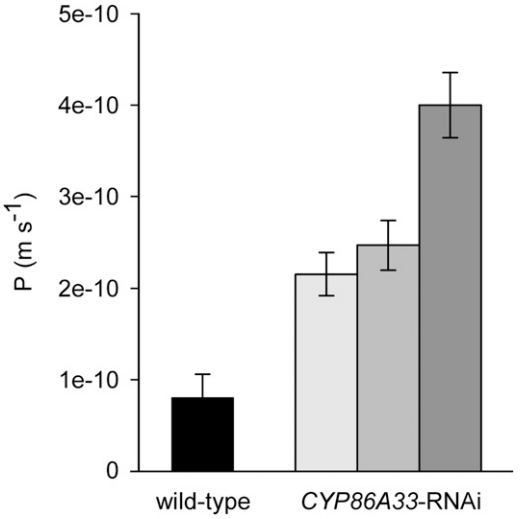

Figure 5. Water permeances of isolated periderms of *CYP86A33*-RNAi and wild type from 21-d-stored tubers. CYP86A33 silencing impairs periderm barrier properties and increases water permeance (*P*; m s^{-1}) in periderms from three independent CYP86A33-RNAi lines ($n = 3$, $n = 3$, and $n = 4$) compared to wild type ($n = 22$). Data represent the mean ± SD.

Significance of ω-Functional Fatty Acids in Suberin Biosynthesis

In wild-type potato periderm, the aliphatic suberin and wax chemical composition was comparable with previous analysis (Schreiber et al., 2005). The most obvious general result of *CYP86A33* silencing was the reduction by 60% of total aliphatic suberin affecting all monomers, but first and foremost C18:1 ω-hydroxyacid (70% decrease) and α,ω-diacid (90% decrease), which are the main monomers in aliphatic potato suberin. This fact, together with a marked drop in C20:0 ω-hydroxyacid and C18:0 and C20:0 α,ω-diacid, emphasizes the importance of CYP86A33 for ω-hydroxylation in periderm, taking into account that ω-hydroxyacids are precursors for the synthesis of α,ω-diacids (Agrawal and Kolattukudy, 1977; Dean and Kolattukudy, 1977). The very minor increases in C22 and C24 ω-hydroxyacid and α,ω-diacid, observed only in 21-d-stored tubers, were not sufficient to compensate for the drop in ω-functionalized fatty acids. Nonetheless, as a consequence of *CYP86A33* silencing, all substance classes other than ω-hydroxyacids and α,ω-diacids were also reduced (Fig. 4). Of note is that glycerol was reduced by 60%. This fact may be a consequence of the interaction between suberin metabolic pathways and/or an impaired capacity to esterify such monomers due to the drop in α,ω-functional groups. On the other hand, neither C18:1 ω-hydroxyacid nor α,ω-diacid was totally omitted in suberin from *CYP86A33*-silenced tubers. This low accumulation of products may be due to residual activity of CYP86A33 or more probably to redundant ω-hydroxylases. The latter explanation seems more probable when we consider that knockout mutants of *CYP86A1* (Li et al., 2007; Hofer et al., 2008) and *CYP86A2* (Xiao et al., 2004) showed low levels of ω-functionalized products in suberin and cutin, respectively. As far as the periderm wax fraction is concerned, representing only 4% of periderm aliphatics, *CYP86A33* down-regulation produced opposite effects in comparison with aliphatic suberin. The total extracted amount of wax was greatly increased. Most free fatty acids, primary alcohols, and ferulate esters were augmented, but not all (Table I; Supplemental Table S2). Such increases may result from the accumulation of some aliphatic precursors that cannot be incorporated into the suberin. However, other mechanisms controlling the synthesis, degradation, and redirection of monomers to other pathways should also be active in periderm.

All members of the CYP86A subfamily in Arabidopsis analyzed so far have a demonstrated fatty acid ω-hydroxylase activity in vitro (Benveniste et al., 1998; Rupasinghe et al., 2007). A fatty acid ω-hydroxylase activity may also be expected for potato CYP86A33 based on the changes that its deficiency produces in the aliphatic suberin composition that mainly concern the ω-functionalized monomers. The fact that aliphatic suberin compounds other than ω-hydroxyacids and diacids were also altered by *CYP86A33* silencing is

not in contradiction with a ω-hydroxylase activity for CYP86A33 because the Arabidopsis *cyp86a1* mutant also produces similar alteration in suberin composition (Li et al., 2007; Hofer et al., 2008). The similarity in suberin phenotype between CYP86A33- and CYP86A1-deficient plants, in conformity with a high amino acid sequence similarity (89%) between both genes (*CYP86A33* and *CYP86A1*), together with the careful selection of an unconserved region for the *CYP86A33*-hpRNAi construct, strengthens the hypothesis that CYP86A33 deficiency is responsible of the alterations observed in *CYP86A33*-RNAi periderm in comparison to wild type. To unequivocally prove that CYP86A33 has ω-hydroxylase activity, we overexpressed the gene in yeast (*Saccharomyces cerevisiae*) and in *Nicotiana benthamiana* and measured the enzymatic activity in isolated microsomes using lauric acid as substrate. However, none of these systems allowed detection of any ability of the gene product to metabolize free fatty acids. Of note is that several authors point out that substrates other than free fatty acids, such as fatty acids activated, linked to glycerol or to the polymer, could be the natural substrates of CYP86A proteins (Cahoon et al., 2002; Beisson et al., 2007; Li et al., 2007; Pollard et al., 2008). Moreover, the possibility that CYP86A33 could also catalyze the complete oxidation of the methyl to the carboxyl group, as reported for CYP94A5 (Le Bouquin et al., 2001) and CYP94C1 (Kandel et al., 2007), cannot be excluded.

ω-Functional Fatty Acids Are Required for the Periderm Fine Structure and Water Barrier Function

Our analysis allowed the measurement of the effects of *CYP86A33* silencing in the sealing properties of periderm cell walls. Both the thickness and the ultrastructure of the suberin layer (Fig. 3, C and D) were greatly affected by CYP86A33 deficiency, as might be expected from the dramatic changes in the amount of periderm lipid and its composition. These results generally conform to the effects of CYP86A2 deficiency in cuticles as shown by the Arabidopsis *att1* mutant, which presents 70% less cutin and a loose cuticle ultrastructure in comparison with wild type (Xiao et al., 2004). A very significant alteration in the suberin ultrastructure in *CYP86A33*-silenced periderm can be deduced from the loss of the typical regular lamellation and the formation of a few short irregular lamellae and conspicuous clumps of electron-dense and electron-translucent material (Fig. 3, C and D). Although it is generally accepted that translucent lamellae correspond to aliphatic zones and dense lamellae to aromatic rich zones (Schmutz et al., 1993, 1996; Graça and Santos, 2007), suberin macromolecular organization has not been clarified (Franke and Schreiber, 2007). There is some evidence to support the hypothesis that the glycerol-α,ω-diacid-glycerol unit is the base for suberin's three-dimensional structure and that the ω-hydroxyacids are pivotal for the connection of the several translucent lamellae of the suberin polyester and the linkage to the aromatics (Arrieta-Baez and Stark, 2006; Graça and Santos, 2006). According to this hypothesis, the leading cause of the changes observed in the suberin ultrastructure of *CYP86A33*-silenced periderm seems to be the great reduction experienced by C18:1 ω-functionalized monomers. An impairment in the formation of glycerol-α,ω-diacid-glycerol units is consistent with a significant decrease in glycerol and thus with the reduction observed in the lamellation and thickness of the suberin wall. Fewer linkages of ω-hydroxyacids to aromatics agrees with a decrease in esterified aromatic monomers and hence with the formation of clumps of dense material and the loss of the typical regular lamellation. However, clarifying the respective role of diacids and ω-hydroxyacids in assembling the suberin macromolecular structure would require a model in which only one type of ω-functional fatty acids was reduced.

The main function of periderm is the protection it affords against water loss. However, the relationship between the periderm lipid coverage and the water transpiration properties is not fully understood (Schreiber et al., 2005). The crucial role of waxes in water-sealing properties of the periderm has been reported by several authors (Soliday et al., 1979; Vogt et al., 1983; Schreiber et al., 2005), but the periderm of *CYP86A33*-RNAi plants provides clear evidence that aliphatic suberin is also relevant for the water permeability of periderm. Although in *CYP86A33*-RNAi periderm the wax load increases by 2-fold, the permeability to water experiences a 3.5-fold raise, which can be attributed to the marked reduction in aliphatic suberin monomers (a 60% decrease) and the altered ultrastructure of the suberin. Both the monomer's load and the structural organization of the lipid polyester determine the suberin sealing properties. Our results are in general agreement with cutin mutants in which a 60% to 70% reduction in cutin load, accompanied by a distortion in cutin ultrastructure, leads to an increase (from 2- to 4-fold) in permeability to water (Xiao et al., 2004; Li et al., 2007). A relationship between the aliphatic suberin load and permeability to water was suggested by increased permeability to tetrazolium salt of the seed coat of *gpat5* defective in suberin (Beisson et al., 2007). The seed coats of *gpat5* displayed a more fragile appearance and break easily when handled as occurs in periderm from *CYP86A33*-silenced plants. That not only the lipid amount, but also the structural features of the polymer, should be significant for the sealing properties is supported by observations in the cuticle of plants co-overexpressing *GPAT5*/*CYP86A1*, which shows a higher load of aliphatic monomers, but also increased permeability to water (Li et al., 2007).

MATERIALS AND METHODS

Plant Material and Growth Conditions

Potato (*Solanum tuberosum 'Desirée'*) plants were propagated in vitro and tubers were grown in the greenhouse. For in vitro propagation, stem cuttings were cultured in Murashige and Skoog medium (Duchefa) supplemented

with 2% (w/v) Suc and grown in growth cabinets under a light/dark photoperiod cycle of 16/8 h at 22°C and 67 μmol m^{-2} s^{-1}. In vitro plants were transferred to soil and grown for about 2 months in the greenhouse for tuber production. Tubers were harvested from 8-week-old plants and stored at room temperature before analysis.

Cloning of the Full-Length *CYP86A32* and *CYP86A33* Sequences

The full-length of *CYP86A32* (accession no. EU293406) was obtained from the cork oak ESTs EE743846, EE745211, and EE743708 (Soler et al., 2007) by 5′- and 3′-RACE (Invitrogen) according to the manufacturer's protocols. Gene-specific primers 5′-TCAGGGTCAAACAGAAGGA-3′ and 5′-GGGTGACATGTGACAGTGAA-3′ were used to amplify the 5′-end and 5′-AGCGAAGTGGATCGAGAAG-3′ to amplify the 3′-end sequences. The PCR products were cloned into pCR4-TOPO (Invitrogen) and sequenced using the BigDye Terminator 3.1 kit (Applied Biosystems). The full-length *CYP86A33* (accession no. EU293405) was obtained by TBLASTX analysis at the TIGR potato database (http://www.tigr.org) using the cork oak *CYP86A32* sequence as a query. Tentative consensus TC114700 was the best match. The *CYP86A33* sequence was PCR amplified from a cDNA tuber skin, using the gene-specific primers 5′-CACATTGAAAATTACAACAAAGCA-3′ and 5′-TCCTCTCTACTTCACTTAAACCAAAA-3′. First-strand cDNA was synthesized using the SuperScript II reverse transcriptase (Invitrogen) and an oligo $(dT)_{16}$ primer. PCR was carried out using Advantage Polymerase (Promega). *CYP86A32* and *CYP86A33* were named according to the P450 Nomenclature Committee (http://drnelson.utmem.edu/CytochromeP450.html).

Plasmid Construction

The silencing of *CYP86A33* in potato plants was carried out by means of a 224-bp fragment that encompasses nucleotides 1220 to 1443. This fragment was PCR amplified from the BQ513101 clone (Arizona Genomics Institute) using primers 5′-TTTACTCGGTGGGGAGAATG-3′ and 5′-CGGTAATAGCCGGTAACGAA-3′ bearing at their 5′-ends the *attB1* and *attB2* recombinant sequences, respectively. The PCR product was cloned into the donor plasmid pDONR207 (Invitrogen) by BP clonase II recombination (Gateway Technology; Invitrogen). The binary destination vector (pBIN19RNAi) was obtained by subcloning the Gateway RNAi cassette from pH7GWIWG2(II) (www.psb.rug.ac.be/gateway; Karimi et al., 2002) into the pBIN19 vector. For this purpose, the RNAi cassette was excised by a partial *Xba*I digestion and a *Hin*dIII digestion, and inserted into the *Xba*I-*Hin*dIII sites of the pBIN19 plasmid. This cassette included a chloramphenicol resistance marker (*CmR*) and two *ccdB* genes flanked by recombinant *attR1* and *attR2* sequences in inversed orientations, separated by an intron. The *CYP86A33* fragment from pDONR207 was transferred into the binary destination vector using LR clonase II (Invitrogen). The PCR insert and vector were incubated for 5 min at 65°C before the clonase was added to improve cloning efficiency and incubated overnight at room temperature. Recombination replaced the *ccdB* genes by the *CYP86A33* fragment, yielding a hairpin construct able to trigger *CYP86A33* mRNA degradation. Restriction enzyme digestion was used to verify the recombinant construct.

Plant Transformation for RNAi-Mediated Silencing

Potato leaves were infected with the *Agrobacterium tumefaciens* strain GV2260 transformed with the RNAi recombinant plasmid in accordance with Hofgen and Willmitzer (1988). Potato cv *Desirée* plants were transformed as previously described by Banerjee et al. (2006). Kanamycin-resistant plants were regenerated and grown until tuber development and analyzed for *CYP86A33* mRNA accumulation in the tuber skin.

RNA Isolation and Northern Analysis

Total RNA was isolated from potato tissues using the guanidine hydrochloride method (Logemann et al., 1987). Samples (20 μg/lane) were separated in a 1.5% formaldehyde-agarose gel (w/v) and transferred onto a nylon membrane (Hybond-N; GE Healthcare). Hybridization was carried out in accordance with Amasino (1986). Filters were hybridized at 42°C and washed in 3× SSC and 0.5% SDS at 65°C. The *CYP86A33*-RNAi fragment was used to obtain a *CYP86A33* probe that was ^{32}P-labeled (GE Healthcare) by the random-primed method (Roche).

RT-PCR with Incremental Cycle Numbers

We followed the procedure described by Soler et al. (2007). For each tissue analyzed, first-stranded cDNA was synthesized from 0.5 μg of total RNA using Superscript III (Invitrogen) in a 20-μL reaction and then 2.5-fold diluted. The total RNA used was previously treated with TURBO DNase (Ambion) to prevent genomic contamination and a further purification step was performed with the CleanUp protocol of RNeasy plant mini kit (Qiagen). For PCRs to be compared, we used 60-μL reactions with equal amounts of cDNA as a template and forward and reverse gene-specific primers, respectively, for the housekeeping *ACTIN* (TC119084; 5′-CCTTGTATGCTAGTGGTCG-3′ and 5′-GCTCATAGTCAAGAGCCAC-3′), for *CYP86A33* (5′-TCTACTGGGGTATCCGCAAC-3′ and 5′-TTTGGTGAAAGGGTTTCAGG-3′) and for BQ514437 (5′-CAGGGCGTGATACGACTAGC-3′ and 5′-TACGAAGGCTCGTGCCTAAT-3′). Aliquots of 15 μL were taken every three cycles from cycle 30 to 36 and analyzed by agarose gel electrophoresis stained by ethidium bromide. To discard possible genomic DNA contaminations, the actin primers were designed complementary to two exons flanking an intron.

Isolation of Periderm Membranes

Freshly harvested tubers between 3 and 8 cm long were rinsed in tap water and stored for 21 and 60 d at room temperature, in the dark, if necessary. Periderms were isolated enzymatically as described (Vogt et al., 1983; Schreiber et al., 2005). Periderm discs were punched out from tubers using a cork borer (1-cm diameter) and immersed in a mixture of 2% (v/v) cellulase (Celluclast; Novo Nordiskand) and 2% (v/v) pectinase (Trenolin Super DF; Erbslöh) in 10^{-2} M citric buffer, pH 3.0 (adjusted with KOH). Sodium azide (Sigma) was added to prevent bacterial growth. During the 4-d incubation, the solution was changed two to three times until it was clear. Isolated periderm membranes were washed twice in 2×10^{-2} M boric buffer, pH 9.0, for 24 h and then carefully washed with deionized water. All incubations were carried out at room temperature with shaking at 30 rpm. Isolated periderms were dried and stored at room temperature until used.

In a strict sense, potato periderm is composed of three distinct tissues: the suberized tissue (phellem), the cambial layer (phellogen), and the phelloderm. During this enzymatic isolation, only the suberized phellem tissue is obtained, whereas phellogen and phelloderm are removed. However, we use the term periderm instead of phellem as a number of different authors have done in the past (Vogt et al., 1983; Stark et al., 1994; Schreiber et al., 2005).

Measurement of Peridermal Permeance

Peridermal permeability was measured using a gravimetric method previously described (Schönherr and Lendzian, 1981; Schreiber et al., 2005). Isolated periderm membranes were soaked overnight in deionized water, laid flat on plastic sheets, and left to dry at room temperature for 24 h. To avoid the effect of lenticels on water permeability measurements, small chambers (diameter 6 mm) and periderm fragments free of lenticels were used. Periderm membranes were mounted on water-filled transpiration chambers (300 μL) made of stainless steel with the physiological inner side of the isolated periderm facing the inner side of the chambers. Once mounted, the transpiration chambers were turned upside down to ensure direct contact between water and periderm. Chambers were kept in closed polyethylene boxes containing dry silica gel and stored at 25°C and the weight loss caused by evaporation of water across the periderm to the silica gel was determined at regular intervals using an analytical balance (Analytic AC210S; Sartorius). Transpiration kinetics was obtained by plotting the amounts of water (g), which had diffused across the periderm, against time (s). Permeances (P; m s^{-1}) were calculated from the slopes (F; g s^{-1}) of the linear regression lines and fitted to the transpiration kinetics using the following equation: $P = F \times (A \times \Delta c)^{-1}$, where A (2.83×10^{-3} m^2) corresponds to the exposed area and Δc (10^6 g m^{-3}) represents the driving force, provided by the concentration of water in the chamber (Schreiber et al., 2005).

GC Analysis

Wax and aliphatic suberin extraction and GC-mass spectrometry (MS) and GC-flame ionization detector (FID) analysis were carried out as previously described (Schreiber et al., 2005). The total amount of periderm material used for each analysis ranged from 2 to 3 mg. Three independent *CYP86A33* down-regulated lines were used for these studies. Wax was extracted from isolated

periderms at room temperature for 18 h in a mixture (1:1 [v/v]) of chloroform and methanol. Chloroform-methanol extracts were used for wax analysis without further purification. For the depolymerization of aliphatic suberin, wax-free periderms were dried for at least 24 h in a desiccator containing silica gel, and subsequently transesterified by incubation at 70°C for 18 h with methanol-boron trifluoride (approximately 10% BF3 in methanol; Fluka; Kolattukudy and Agrawal, 1974; Zeier and Schreiber, 1998). Monomers released after transesterification and wax extracts obtained by chloroform-methanol extraction were analyzed as trimethylsilyl (TMS) derivatives by means of GC-MS and GC-FID. TMS derivatives were prepared after complete solvent evaporation (N_2 gas) by adding 100 μL of chloroform, and derivatized with a 1:1 (v/v) mixture of 20 μL pyridine (GC grade; Merck) and 20 μL of *N,N*-bis-trimethylsilyltrifluoroacetamide (Macherey-Nagel) for 40 min at 70°C. Monomers were quantified using a GC-FID (HP 5890 Series II; Hewlett-Packard) and analyzed using HPChemStation software (Hewlett-Packard) by comparison with an internal standard (2 μg of tetracosane for wax and 10 μg dotriacontane for suberin). Identification of the compounds was carried out by GC and a quadrupole mass selective detector HP 5971A (Hewlett-Packard) as described previously (Schreiber et al., 2005).

Determination of Glycerol

The glycerol content in suberin was enzymatically quantified based on the method reported in the past (Schmutz et al., 1996; Moire et al., 1999). Prior to analysis, periderm membranes were treated with a chloroform-methanol mixture as described above. Then wax-free periderm membranes were transesterified at 70°C for 18 h with methanol-boron trifluoride (approximately 10% BF3 in methanol; Fluka) to release the aliphatic suberin compounds. The hydrolyzed cell wall residues were rinsed once with chloroform. The methanolysate were neutralized with saturated sodium hydrogen carbonate and the aqueous phase selected for the determination of glycerol. Free glycerol was quantified at 540 nm using the free glycerol reagent (Sigma) and a glycerol standard solution (triolein; Sigma). All three independent *CYP86A33* down-regulated lines were used for this study.

Sequence Alignment and Phylogenetic Analysis

Amino acid sequence alignments were performed using the ClustalW program at the European Bioinformatics Institute (EBI; http://www.ebi.ac.uk/Tools/clustalw). The alignment was edited using the BioEdit Sequence Alignment Editor 7.0.1 (Hall, 1999). CYP86A SRSs and the amino acidic residues predicted to contact the oleic acid substrate were identified in accordance with Rupasinghe et al. (2007). Phylogenetic analyses were conducted using MEGA, version 3.1 (Kumar et al., 2004).

Periderm Microscopy

For light and fluorescence microscopy, small fragments of tuber periderm and isolated periderm discs were included in fresh potato blocks and cut using a rotation microtome (Anglia Scientific). Sections were mounted on slides in water and observed in bright field and epifluorescence on a Leica DMR-XA optical microscope (Leica Microsystems).

For SEM, small fragments of tuber periderm were fixed under vacuum with 4% formaldehyde in phosphate-buffered saline (pH 7.5) at room temperature for at least 48 h. Fragments were dehydrated with an increasing ethanol concentration series exchanged through amyl-acetate and critical point dried. The pieces were mounted on copper stubs and coated with gold. Specimens were observed using a Zeiss DSM 960A SEM (Zeiss). Digital images were collected and processed using the Quartz PCI 5.10 (Quartz Imaging Corporation).

For TEM, sections of periderm dissected into 1×1 mm^2 were immediately placed in 100 mM sodium cacodylate buffer (pH 7.0) containing 2.5% (w/v) glutaraldehyde and 2% (w/v) paraformaldehyde for 2 to 4 h. A vacuum was applied until samples were submerged. Tissues were washed three times with 100 mM sodium cacodylate buffer (pH 7.0) and subsequently fixed overnight in 100 mM sodium cacodylate buffer (pH 7.0) containing 1% (w/v) osmium tetroxide. Samples were then washed with 100 mM sodium cacodylate buffer (pH 7.0), dehydrated in an acetone series (30%–100% by 10% steps, 10 min each step), and infiltrated with Spurr's epoxy resin (1:2, 1:1, and 2:1 resin: acetone [v/v] and pure resin for 4 h, overnight, 3 and 5 h, respectively). Infiltrated tissues were placed in molds and incubated at 60°C for 2 d. Embedded materials were thin sectioned using an ultramicrotome RMC MT-XL Sections were collected onto 200-mesh copper grids, stained with 2% (w/v) uranyl acetate for 15 min and rinsed for 30 min before being observed and photographed with the TEM ZEISS EM910 (Germany) at an accelerating voltage of 60 kV. Images were obtained on Kodak Electron Microscope film 4489 and scanned by HP 6100C (Hewlett-Packard).

All microscopic analyses were performed by the microscopy service of the University of Girona.

CYP86A32 (accession no. EU293406) and *CYP86A33* (accession no. EU293405) have been isolated in this work. Three cork oak ESTs (accession nos. EE743846, EE745211, and EE743708) were used to obtain the full-length sequence of *CYP86A32*. The sequences CYP86A1 (accession no. NP_200694), CYP86A2 (accession no. NP_191946), CYP86A4 (accession no. NP_171666), CYP86A7 (accession no. NP_176558), CYP86A8 (accession no. NP_182121), CYP86A9 (accession no. AP003442), CYP86A10 (accession no. AP004139), CYP86A11 (accession no. AL606687) and CYP94C1 (accession no. NP_180337) were used to construct the phylogenetic tree.

Supplemental Data

The following materials are available in the online version of this article.

Supplemental Figure S1. Analysis of the putative off-target EST BQ514437 in *CYP86A33*-RNAi periderm.

Supplemental Figure S2. *CYP86A33*-RNAi aliphatic suberin chemical composition at different stages of tuber maturation.

Supplemental Figure S3. Water permeances of isolated periderms of *CYP86A33*-RNAi and unsilenced or control periderms from 60-d-stored tubers.

Supplemental Table S1. List of the potato ESTs most homologous to *CYP86A33*-RNAi fragment.

Supplemental Table S2. Wax chemical composition of *CYP86A33*-RNAi periderm at different stages of tuber maturation.

ACKNOWLEDGMENTS

We would like to thank to Jordi Blavia and Carme Carulla (Serveis Tècnics de Recerca, Universitat de Girona) for their highly skilled work with TEM and SEM; Dr. Pilar Fontanet (Institut de Biologia Molecular de Barcelona) for helpful advice on potato treatments; and Imma Guardiola and Sara Gómez (Departament de Biologia, Universitat de Girona) for taking care of the transgenic plants.

Received July 30, 2008; accepted December 18, 2008; published December 24, 2008.

LITERATURE CITED

Agrawal VP, Kolattukudy PE (1977) Biochemistry of suberization—ω-hydroxyacid oxidation in enzyme preparations from suberizing potato-tuber disks. Plant Physiol **59:** 667–672

Altschul SF, Gish W, Miller W, Myers EW, Lipman DJ (1990) Basic local alignment search tool. J Mol Biol **215:** 403–410

Amasino RM (1986) Acceleration of nucleic-acid hybridization rate by polyethylene-glycol. Anal Biochem **152:** 304–307

Arrieta-Baez D, Stark RE (2006) Using trifluoroacetic acid to augment studies of potato suberin molecular structure. J Agric Food Chem **54:** 9636–9641

Banerjee AK, Prat S, Hannapel DJ (2006) Efficient production of transgenic potato (*S. tuberosum* L ssp andigena) plants via *Agrobacterium tumefaciens*-mediated transformation. Plant Sci **170:** 732–738

Beisson F, Li Y, Bonaventure G, Pollard M, Ohlrogge JB (2007) The acyltransferase GPAT5 is required for the synthesis of suberin in seed coat and root of *Arabidopsis*. Plant Cell **19:** 351–368

Benveniste I, Tijet N, Adas F, Philipps G, Salaun JP, Durst F (1998) *CYP86A1* from *Arabidopsis thaliana* encodes a cytochrome P450-dependent fatty acid omega-hydroxylase. Biochem Biophys Res Commun **243:** 688–693

Bernards MA (2002) Demystifying suberin. Can J Bot **80:** 227–240

Cahoon EB, Ripp KG, Hall SE, McGonigle B (2002) Transgenic production of epoxy fatty acids by expression of a cytochrome P450 enzyme from *Euphorbia lagascae* seed. Plant Physiol **128:** 615–624

Dean BB, Kolattukudy PE (1977) Biochemistry of suberization—incorporation of [1-^{14}C]oleic acid and [1-^{14}C]acetate into aliphatic components of suberin in potato-tuber disks (*Solanum tuberosum*). Plant Physiol **59:** 48–54

Duan H, Schuler MA (2005) Differential expression and evolution of the Arabidopsis CYP86A subfamily. Plant Physiol **137:** 1067–1081

Esau K (1965) Plant Anatomy, Ed 2. John Wiley & Sons, New York, pp 366–381

Franke R, Schreiber L (2007) Suberin—a biopolyester forming apoplastic plant interfaces. Curr Opin Plant Biol **10:** 252–259

Graça J, Pereira H (2000) Suberin structure in potato periderm: glycerol, long-chain monomers, and glyceryl and feruloyl dimers. J Agric Food Chem **48:** 5476–5483

Graça J, Santos S (2006) Linear aliphatic dimeric esters from cork suberin. Biomacromolecules **7:** 2003–2010

Graça J, Santos S (2007) Suberin: a biopolyester of plants' skin. Macromol Biosci **7:** 128–135

Hall TA (1999) BioEdit: a user-friendly biological sequence alignment editor and analysis program for Windows 95/98/NT. Nucleic Acids Symp Ser **41:** 95–98

Hofer R, Briesen I, Beck M, Pinot F, Schreiber L, Franke R (2008) The Arabidopsis cytochrome P450 *CYP86A1* encodes a fatty acid ω-hydroxylase involved in suberin monomer biosynthesis. J Exp Bot **59:** 2347–2360

Hofgen R, Willmitzer L (1988) Storage of competent cells for Agrobacterium transformation. Nucleic Acids Res **16:** 9877

Kandel S, Sauveplane V, Compagnon V, Franke R, Millet Y, Schreiber L, Werck-Reichhart D, Pinot F (2007) Characterization of a methyl jasmonate and wounding-responsive cytochrome P450 of *Arabidopsis thaliana* catalyzing dicarboxylic fatty acid formation in vitro. FEBS J **274:** 5116–5127

Karimi M, Inze D, Depicker A (2002) GATEWAY vectors for Agrobacterium-mediated plant transformation. Trends Plant Sci **7:** 193–195

Kolattukudy PE (1980) Biopolyester membranes of plants—cutin and suberin. Science **208:** 990–1000

Kolattukudy PE (2001) Polyesters in higher plants. Adv Biochem Eng Biotechnol **71:** 1–49

Kolattukudy PE, Agrawal VP (1974) Structure and composition of aliphatic constituents of potato-tuber skin (suberin). Lipids **9:** 682–691

Kumar S, Tamura K, Nei M (2004) MEGA3: integrated software for molecular evolutionary genetics analysis and sequence alignment. Brief Bioinform **5:** 150–163

Le Bouquin R, Skrabs M, Kahn R, Benveniste I, Salaun JP, Schreiber L, Durst F, Pinot F (2001) CYP94A5, a new cytochrome P450 from Nicotiana tabacum is able to catalyze the oxidation of fatty acids to the ω-alcohol and to the corresponding diacid. Eur J Biochem **268:** 3083–3090

Li Y, Beisson F, Koo AJK, Molina I, Pollard M, Ohlrogge J (2007) Identification of acyltransferases required for cutin biosynthesis and production of cutin with suberin-like monomers. Proc Natl Acad Sci USA **104:** 18339–18344

Logemann J, Schell J, Willmitzer L (1987) Improved method for the isolation of RNA from plant tissues. Anal Biochem **163:** 16–20

Lulai EC, Freeman TP (2001) The importance of phellogen cells and their structural characteristics in susceptibility and resistance to excoriation in immature and mature potato tuber (*Solanum tuberosum* L) periderm. Ann Bot (Lond) **88:** 555–561

Lulai EC, Weiland JJ, Suttle JC, Sabba RP, Bussan AJ (2006) Pink eye is an unusual periderm disorder characterized by aberrant suberization: a cytological analysis. Am J Potato Res **83:** 409–421

Moire L, Schmutz A, Buchala A, Yan B, Stark RE, Ryser U (1999) Glycerol is a suberin monomer. New experimental evidence for an old hypothesis. Plant Physiol **119:** 1137–1146

Nawrath C (2002) The biopolymers cutin and suberin. *In* C Somerville, EM Meyerowitz, eds, The Arabidopsis Book. American Society of Plant Biologists, Rockville, MD, doi/101199/tab0021

Nelson DR, Schuler MA, Paquette SM, Werck-Reichhart D, Bak S (2004) Comparative genomics of rice and Arabidopsis. Analysis of 727 cytochrome P450 genes and pseudogenes from a monocot and a dicot. Plant Physiol **135:** 756–772

Pollard M, Beisson F, Li Y, Ohlrogge JB (2008) Building lipid barriers: biosynthesis of cutin and suberin. Trends Plant Sci **13:** 236–246

Rupasinghe SG, Duan H, Schuler MA (2007) Molecular definitions of fatty acid hydroxylases in *Arabidopsis thaliana*. Proteins **68:** 279–293

Sabba RP, Lulai EC (2002) Histological analysis of the maturation of native and wound periderm in potato (*Solanum tuberosum* L) tuber. Ann Bot (Lond) **90:** 1–10

Schmidt HW, Schönherr J (1982) Fine-structure of isolated and non-isolated potato-tuber periderm. Planta **154:** 76–80

Schmutz A, Buchala AJ, Ryser U (1996) Changing the dimensions of suberin lamellae of green cotton fibers with a specific inhibitor of the endoplasmic reticulum-associated fatty acid elongases. Plant Physiol **110:** 403–411

Schmutz A, Jenny T, Amrhein N, Ryser U (1993) Caffeic acid and glycerol are constituents of the suberin layers in green cotton fibres. Planta **189:** 453–460

Schönherr J, Lendzian K (1981) A simple and inexpensive method of measuring water permeability of isolated plant cuticular membranes. Z Pflanzenphysiol **102:** 321–327

Schreiber L, Franke R, Hartmann K (2005) Wax and suberin development of native and wound periderm of potato (*Solanum tuberosum* L) and its relation to peridermal transpiration. Planta **220:** 520–530

Soler M, Serra O, Molinas M, Garcia-Berthou E, Caritat A, Figueras M (2008) Seasonal variation in transcript abundance in cork tissue analyzed by real time RT-PCR. Tree Physiol **28:** 743–751

Soler M, Serra O, Molinas M, Huguet G, Fluch S, Figueras M (2007) A genomic approach to suberin biosynthesis and cork differentiation. Plant Physiol **144:** 419–431

Soliday CL, Kolattukudy PE, Davis RW (1979) Chemical and ultrastructural evidence that waxes associated with the suberin polymer constitute the major diffusion barrier to water-vapor in potato-tuber (*Solanum tuberosum* L). Planta **146:** 607–614

Stark RE, Sohn W, Pacchiano RA, Albashir M, Garbow JR (1994) Following suberization in potato wound periderm by histochemical and solid-state ^{13}C nuclear-magnetic-resonance method. Plant Physiol **104:** 527–533

Vogt E, Schönherr J, Schmidt HW (1983) Water permeability of periderm membranes isolated enzymatically from potato-tubers (*Solanum tuberosum* L). Planta **158:** 294–301

Wellesen K, Durst F, Pinot F, Benveniste I, Nettesheim K, Wisman E, Steiner-Lange S, Saedler H, Yephremov A (2001) Functional analysis of the *LACERATA* gene of Arabidopsis provides evidence for different roles of fatty acid omega-hydroxylation in development. Proc Natl Acad Sci USA **98:** 9694–9699

Xiao F, Goodwin SM, Xiao Y, Sun Z, Baker D, Tang X, Jenks MA, Zhou JM (2004) Arabidopsis *CYP86A2* represses Pseudomonas syringae type III genes and is required for cuticle development. EMBO J **23:** 2903–2913

Zeier J, Schreiber L (1998) Comparative investigation of primary and tertiary endodermal cell walls isolated from the roots of five monocotyledoneous species: chemical composition in relation to fine structure. Planta **206:** 349–361